


Magnetic field induced deformation of the spin density wave microphases in $\text{Ca}_3\text{Co}_2\text{O}_6$ Y. Kamiya *School of Physics and Astronomy, Shanghai Jiao Tong University, Shanghai 200240, China*

(Received 3 December 2021; revised 25 November 2022; accepted 18 January 2023; published 10 April 2023)

The frustrated triangular Ising magnet $\text{Ca}_3\text{Co}_2\text{O}_6$ has long been known for an intriguing combination of extremely slow spin dynamics and peculiar magnetic orders, such as the evenly spaced nonequilibrium metamagnetic magnetization steps and the long-wavelength spin density wave (SDW) order, the latter of which is essentially an emergent crystal of solitons. Recently, an elaborate field-cooling protocol to bypass the low-field SDW phase was proposed to overcome the extraordinarily long timescale of spin relaxation that impeded previous experimental studies in equilibrium, which may point to a deep connection between the low-temperature slow relaxation and the cooling process passing through the low-field SDW phase. As the first step to elucidate the conjectured connection, we investigate the magnetic field induced deformation of the SDW state and incommensurate-commensurate transitions, thereby mapping out the equilibrium in-field phase diagram for a realistic three-dimensional lattice spin model by using Monte Carlo simulations. We also discuss Ginzburg-Landau theory that includes several umklapp terms as well as an effective sine-Gordon model, which can qualitatively explain the observed magnetic field induced deformation of the SDW microphases.

DOI: [10.1103/PhysRevB.107.134409](https://doi.org/10.1103/PhysRevB.107.134409)**I. INTRODUCTION**

Frustrated magnets can have a manifold of nearly degenerate low-energy states from which interesting phenomena may emerge, such as exotic magnetic and nonmagnetic orders, topological order, liquidlike, or even glassy behavior, and so on, varying from one material to another [1]. Even a classical system can host unconventional quasiparticles, such as skyrmions [2], solitons, and monopoles in spin ice [3–5], and they may crystallize into novel spin textures, such as skyrmion crystals [6,7] or soliton crystals [8,9]. Such emergent crystalline states can often be sensitive to external perturbations, which makes them attractive as potential devices in some cases [10]. They can also provide a platform to study far-from-equilibrium dynamics due to metastable states [4,11].

Since the late 1990s [12–15] the frustrated triangular Ising magnet $\text{Ca}_3\text{Co}_2\text{O}_6$ (CCO) has long been known for an intriguing combination of extremely slow spin dynamics and peculiar magnetic phases, such as metamagnetic magnetization steps and an incommensurate spin-density wave (SDW) state [16–22], the latter of which can be seen as a soliton crystal [23]. In CCO, trigonal prismatic Co^{3+} $S = 2$ sites form ferromagnetic Ising chains running along the c axis, whereas arranged in a triangular lattice on the ab plane coupled by weak antiferromagnetic interactions (Fig. 1) [24]. Below spin-freezing temperature $T_{\text{SF}} \simeq 5$ K, CCO exhibits striking evenly spaced metamagnetic magnetization steps [14], whose origin has been a subject of long-time debates [14,15,19,25–28]. Interestingly, whereas the step heights are sensitive to protocol details, such as sweep rate of the external magnetic field, the transition magnetic fields ($\simeq 1.2, 2.4,$ and 3.6 T with additional steps at higher fields) are rather robust [26]. Although

some theory invoked an analogy with quantum tunneling in molecular magnets [27], an alternative scenario is that peculiar frustration in CCO causes a nonequilibrium phenomenon [11]. In the so-called “rigid chain” model [29–34] each ferromagnetic chain is replaced by an effective Ising spin on a two-dimensional antiferromagnetic triangular lattice. Based on this mapping, it was argued that the metamagnetic transition steps in CCO may arise from the same kind of degenerate manifold as in the two-dimensional triangular lattice Ising model [11].

However, the origin of the slow dynamics can be more intricate than suggested by the rigid chain picture. More recently, resonant x-ray [16,17] and neutron spectroscopies [18–22] revealed the SDW order below $T_{\text{SDW}} \simeq 25$ K, which has a three-sublattice structure and a very long modulation wavelength $\lambda_{\text{SDW}} \simeq 10^3$ Å ($\simeq 10^2$ magnetic sites) along the c axis. It was found that λ_{SDW} increases as temperature T is lowered and the corresponding relaxation time grows substantially. Eventually, the system starts to deviate from equilibrium below $T \lesssim 13$ K [19], which is much higher than T_{SF} for the appearance of the metamagnetic magnetization steps. Since the spin chains are not ferromagnetically ordered in the SDW state, the interpretation of the rigid chain picture can be more subtle than originally proposed.

Indeed, the SDW phase may hold the key to understanding the peculiar slow dynamics at low temperatures. It was recently demonstrated that the slow spin dynamics can be bypassed by an elaborate field-cooling protocol where every in-field measurement is performed after a separate cooling in the target magnetic field [35]. Remarkably, the protocol allowed for reaching the 1/3 magnetization plateau down to $T = 2$ K $< T_{\text{SF}}$ without being suffered from metastable states, which was in good agreement with Monte Carlo (MC)

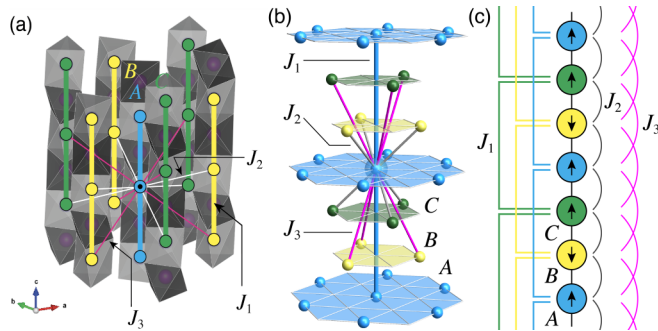


FIG. 1. (a) Magnetic lattice of CCO with the intrachain coupling J_1 and the interchain couplings J_2 and J_3 , which is superimposed on the schematic crystal structure with sublattices A , B , and C . (b) Another schematic for the magnetic lattice where only those exchange interactions that connect to the central site are shown to illustrate them in a concise manner. (c) Effective one-dimensional lattice used in the mean-field theory (see the text), where an arrow represents a magnetic moment of a given ab plane.

simulations in equilibrium. Since the SDW order is believed to disappear and is replaced by a ferrimagnetic state at high magnetic fields, the new experiment may suggest that the spin relaxation at low temperatures may be influenced by the extent to which the system is in the low-field SDW phase during the cooling. In fact, it is known that the SDW order is accompanied by short-range order indicative of spin disordering, whose spectral weight increases as T is lowered [36]. This unusual behavior could be due to the combination of the T -dependent ordering wave vector and the slowness in the relaxation of the system to follow the variation [19].

The observed SDW state is essentially a soliton crystal as in the axial next-nearest-neighbor Ising (ANNNI) model [23], a prototypical model for spontaneous superstructures due to competition between nearest- and next-nearest-neighbor Ising interactions in one direction of a square or cubic lattice [8,9]. The T -dependent change in λ_{SDW} [19] corresponds to different magnetic *microphases* [23], similar to other self-organizing modulated phases in physical and chemical systems [37]. Thus, CCO may provide a rare intersection where the ANNNI model phenomenology [8,9] meets out-of-equilibrium physics in a solid-state system with only short-range interactions. To elucidate this conjecture in CCO and similar materials, such as $\text{Ca}_3\text{Co}_{2-x}\text{Mn}_x\text{O}_6$ [28], $\text{Sr}_2\text{Ca}_2\text{CoMn}_2\text{O}_9$ [38], and $\text{Ca}_3\text{CoRhO}_6$ [39], it is important to investigate the magnetic field induced deformation of the SDW state and incommensurate-commensurate (IC-C) transitions under the condition much closer to equilibrium than ever reached before. To provide a theoretical guide for such an experiment, we study an equilibrium in-field phase diagram of a realistic three-dimensional (3D) lattice model for CCO. We address both model-specific and universal physics by combining mean-field theory (Sec. III), MC simulations (Sec. IV), and Ginzburg-Landau (GL) theory (Sec. V).

II. MODEL

In CCO, $S = 2$ spins have large easy-axis anisotropy [14], which permits a description by an effective classical Ising

model,

$$\hat{H} = \sum_{v=1-3} \sum_{\langle ij \rangle_v} J_v \sigma_i^z \sigma_j^z - h \sum_i \sigma_i^z, \quad (1)$$

where $\sigma_i^z = \pm 1$, $h = g\mu_B S H$ with g , μ_B , and H being the g factor, the Bohr magneton, and a magnetic field, respectively, and $\langle ij \rangle_v$ denotes neighboring sites connected by J_v , $v \in \{1-3\}$. $J_1 < 0$ is the intrachain ferromagnetic interaction and J_2 (J_3) is the antiferromagnetic interchain interaction shifted by $1/3$ ($2/3$) lattice parameters along the c axis (Fig. 1). An *ab initio* study suggested $|J_1| \gg J_2 \simeq J_3$ [40] and $J_1 = -23.9(2)$ and $J_2 + J_3 = 2.3(2)$ K was reported by an NMR experiment, which further suggested $J_2 = 1.1$ and $J_3 = 1.2$ K to explain the SDW ordering wave vector [41]. Below, for simplicity, we assume $J_2/|J_1| = J_3/|J_1|$ and denote the ratio by κ ; in relation with CCO, $\kappa \simeq 0.048$.

III. MEAN-FIELD THEORY

In CCO, J_2 and J_3 compete with J_1 after a few steps along a spiral path due to the vertical shifts of the interchain interactions [42]. This spiral structure is the key to realize the same kind of geometrical frustration as in the ANNNI model [8,9] despite the apparent structural differences. We first briefly discuss a heuristic mean-field theory in zero field by assuming a ferromagnetic order on each ab plane, which are separated by $1/3$ lattice parameters from each other along the c axis (Fig. 1) [23]. The mean-field equation for the magnetization m_l of layer l is

$$\langle m_l \rangle = \tanh \beta h_l, \quad (2)$$

where $h_l = -J_1(\langle m_{l+3} \rangle + \langle m_{l-3} \rangle) - 3J_2(\langle m_{l+1} \rangle + \langle m_{l-1} \rangle) - 3J_3(\langle m_{l+2} \rangle + \langle m_{l-2} \rangle)$. In this quasi-one-dimensional description, J_1 , J_2 , and J_3 serve as the effective third-, first-, and second-neighbor interactions, respectively, realizing a very similar situation as in the prototypical ANNNI model [Fig. 1(c)]. The reason for assuming an in-plane ferromagnetic order, even though the interchain interactions J_2 and J_3 are much smaller than the intrachain interaction J_1 , is that the energy scale associated with the competition between SDW states with different wavelengths along the c axis can be even smaller, as will be discussed by using a sine-Gordon model. In Fig. 2(a), we show the mean-field (κ, T) phase diagram, by extending the previous work [23]. Below the SDW transition temperature $T_{\text{SDW}}(\kappa)$, the ordering wave vector $\mathbf{Q} = (0, 0, Q_3)$ varies quasicontinuously. Eventually, there is a lock-in IC-C transition at $T = T_{\text{IC-C}}$, below which the magnetic unit cell of the mean-field solution is $\uparrow\uparrow\downarrow$ or $\downarrow\downarrow\uparrow$ for $\kappa < 1$ and $\uparrow\uparrow\downarrow\downarrow$ for $\kappa > 1$ in the effective one-dimensional description in Fig. 1(c). We find that $Q_3(\kappa, T)$ changes quasicontinuously over almost the entire phase diagram, especially for relatively small κ , corresponding to numerous microphases of soliton crystals [23]. Meanwhile, distinct discontinuous changes in $Q_3(\kappa, T)$ are also seen in the region with relatively large κ where a few relatively extended commensurate states are found. However, since the large κ region has relatively small significance in relation with CCO, we will not go into details of this case.

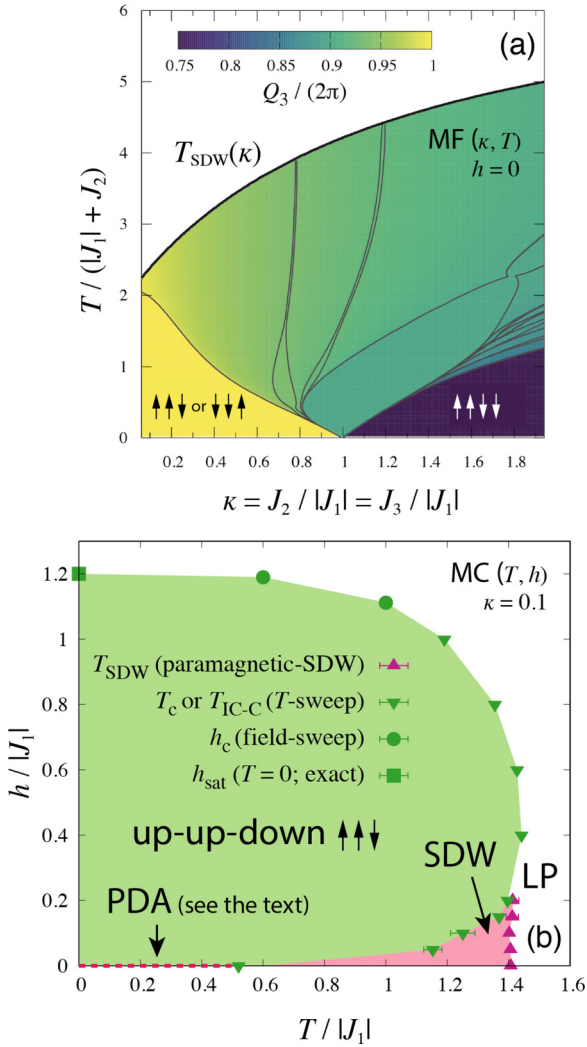


FIG. 2. (a) Mean-field (κ, T) phase diagram for $h = 0$, where $\kappa \equiv J_2/|J_1| = J_3/|J_1|$. The mean-field ground state is $\uparrow\uparrow\downarrow$ or $\downarrow\downarrow\uparrow$ ($\uparrow\uparrow\downarrow\downarrow$) along the c axis for $\kappa < 1$ ($\kappa > 1$) in the effective one-dimensional description, the ordering wave vector of which is $Q_3/(2\pi) = 1$ ($3/4$), respectively. (b) (T, h) phase diagram obtained by MC simulations for $\kappa = 0.1$ based on the data for $T \gtrsim 0.45|J_1|$. The T -sweep data for T_c or T_{IC-C} is determined by analyzing the Binder parameter as a function of T , whereas the field-sweep data for h_c is determined from a peak in $\chi = dM/dh$ as a function of h .

IV. MONTE CARLO SIMULATION

A. Setup

Next, to demonstrate the ANNNI-like physics in an unbiased way, we present the results of our MC simulations. We consider a lattice of size $L \times L \times L_c$ with periodic boundary conditions where the total number of spins is $N_{\text{spin}} = 3L^2L_c$. We combine single-spin updates, intrachain cluster updates [23], and replica exchanges [43] included every ten MC steps. Several hundreds of replicas are needed for largest lattices to maintain a reasonable exchange acceptance rate to guarantee efficient sampling at low temperatures (e.g., 400 replicas for $8 \times 8 \times 320$ for $h \lesssim 0.2|J_1|$). By fixing $\kappa = 0.1$ and $L_c/L = 40$ in most cases shown below, we performed simulations for $2 \times 2 \times 80$ – $8 \times 8 \times 320$. Here, although $\kappa = 0.1$ is larger

than $\kappa \simeq 0.048$ estimated for CCO, no qualitatively different physics for smaller κ is suggested in our mean-field phase diagram as long as the SDW order is concerned [Fig. 2(a)].

The aspect ratio $L_c/L = 40$ is chosen to simulate long-wavelength SDW states with as little finite-size tension as possible whereas not making the system excessively anisotropic to address thermodynamic behaviors in 3D. As will be discussed by using a GL theory, the ordering wave-vector \mathbf{Q} at $T = T_{\text{SDW}}$ is expected to be the minima $\pm\mathbf{q}_{\text{min}}$ of the Fourier-transform $J(\mathbf{q})$ of the exchange interactions, which we find $\mathbf{q}_{\text{min}} = (0, 0, 2\pi + \epsilon)$ with $\epsilon \approx -0.006(2\pi)$ for $\kappa \simeq 0.048$ and $\epsilon \approx -0.013(2\pi)$ for $\kappa = 0.1$. Because \mathbf{q}_{min} is very close to the three-sublattice commensurate wave-vector $\mathbf{q}_{\text{com}} = (0, 0, 2\pi)$, even a single periodicity of the spin modulation requires a large number of unit cells along the c axis. (Here, $\mathbf{q} = 3\mathbf{q}_{\text{com}} = (0, 0, 6\pi)$ is equivalent to $\mathbf{q} = 0$ in our notation, but $\mathbf{q} = \mathbf{q}_{\text{com}}$ is not.) The minimum size required to host a single period modulation for $\kappa \simeq 0.048$ is $L_c^{\text{min}} = 2\pi/|q_{\text{min},3} - q_{\text{com},3}| \approx 160$, which can be a bit problematic. For $\kappa = 0.1$, we find $L_c^{\text{min}} \approx 80$, which is also quite anisotropic but within the acceptable range. The aspect ratio $L_c/L = 40$ is determined on this basis.

B. Modified Binder parameter method

To determine the transition point of a second-order phase transition into a commensurate ordering, say with a wave-vector \mathbf{Q} , a standard method is to analyze the order parameter $M_{\mathbf{Q}} = N_{\text{spin}}^{-1} \sum_i \sigma_i^z \exp(-i\mathbf{Q} \cdot \mathbf{r}_i)$ and the corresponding Binder parameter $U_{\mathbf{Q}} = \langle |M_{\mathbf{Q}}|^4 \rangle / \langle |M_{\mathbf{Q}}|^2 \rangle^2$ [44]. However, the possible T -dependent variation as well as incommensurability of the ordering wave vector poses a challenge in numerical studies of the ANNNI model and its variants [45–47], demanding a modified approach. In such a model, a finite-size system with periodic boundary conditions is expected to develop a spin correlation whose dominant wave vector is necessarily commensurate but near the true ordering wave-vector $\mathbf{Q}(T)$ in the thermodynamic limit. Such an effective ordering wave-vector $\mathbf{Q}_L^{\text{eff}}(T)$ can be detected as a peak in the finite-size spin structure factor $S_{\mathbf{q}} = N_{\text{spin}}(\langle |M_{\mathbf{q}}|^2 \rangle - |M_{\mathbf{q}}|^2)$ and we expect $\lim_{L \rightarrow \infty} \mathbf{Q}_L^{\text{eff}}(T) = \mathbf{Q}(T)$. Indeed, the observed behavior of $\mathbf{Q}_L^{\text{eff}}(T)$ shows relatively small variance with respect to L , supporting this expectation (Fig. 3). Based on the estimate of $\mathbf{Q}_L^{\text{eff}}(T)$, we evaluate $\langle |M_{\mathbf{Q}_L^{\text{eff}}(T)}|^2 \rangle$ and $\langle |M_{\mathbf{Q}_L^{\text{eff}}(T)}|^4 \rangle$, thereby

$$U_{\mathbf{Q}_L^{\text{eff}}} = \frac{\langle |M_{\mathbf{Q}_L^{\text{eff}}(T)}|^4 \rangle}{\langle |M_{\mathbf{Q}_L^{\text{eff}}(T)}|^2 \rangle^2}, \quad (3)$$

which is a Binder parameter defined at $\mathbf{q} = \mathbf{Q}_L^{\text{eff}}(T)$. As in the usual usage of the Binder parameter [44], we look into the crossing point of $U_{\mathbf{Q}_L^{\text{eff}}(T)}$ for different system sizes to evaluate T_{SDW} .

Unlike the conventional approach, however, the wave-vector $\mathbf{q} = \mathbf{Q}_L^{\text{eff}}(T)$ associated with the Binder parameter for one system size can be different from one for another size in this approach. Furthermore, the wave vector can also be T dependent. To analyze the effect of a small deviation of the wave vector from the true (incommensurate) ordering wave-vector \mathbf{Q} , we review the standard scaling theory

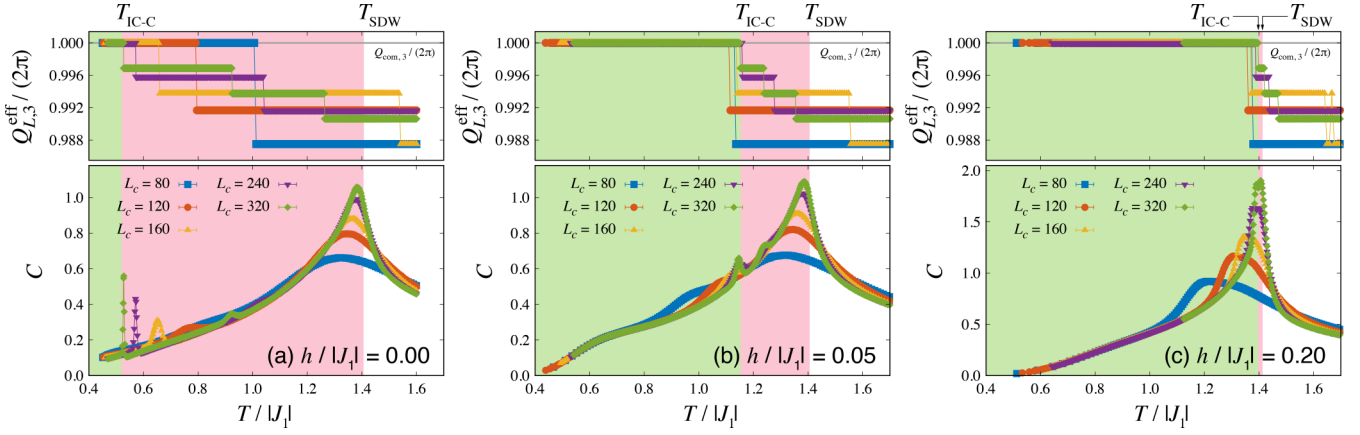


FIG. 3. T dependence of the third component of the effective ordering wave-vector $Q_{L,3}^{\text{eff}}$ (upper panels) and specific heat C (lower panels) obtained by MC simulations for $\kappa = 0.1$ and (a) $h = 0$, (b) $h/|J_1| = 0.05$, and (c) $h/|J_1| = 0.2$. The additional subpeaks in C are considered as spurious ones (see the text).

for correlation functions [48]. The two-point SDW correlation function $G_2(\mathbf{r}_1 - \mathbf{r}_2) = \langle \phi_c(\mathbf{r}_1) \phi_c(\mathbf{r}_2) \rangle$, where $\phi_c(\mathbf{r}) \sim \sigma^z(\mathbf{r}) e^{-i\mathbf{Q}_c \cdot \mathbf{r}}$ is the coarse-grained SDW order parameter with the momentum $\mathbf{Q}_c \equiv \mathbf{Q}(T_{\text{SDW}})$, is expected to have the following transformation under the scaling by a factor b ,

$$G_2(\mathbf{r}, t) \sim b^{-2x_{\text{SDW}}} G_2(b^{-1}\mathbf{r}, b^{1/\nu}t), \quad (4)$$

where $t = (T - T_{\text{SDW}})/T_{\text{SDW}}$ is the reduced temperature, x_{SDW} is the scaling dimension of the order parameter, and ν is the critical exponent of correlation length ξ . It follows that the correlation function has the universal finite-size scaling form of

$$G_2(\mathbf{r}) \sim \xi^{-2x_{\text{SDW}}} \Psi_2(\xi^{-1}\mathbf{r}, \xi^{-1}L), \quad (5)$$

from which we find

$$\begin{aligned} \langle |M_{\mathbf{q}}|^2 \rangle &\sim \frac{1}{N_{\text{spin}}^2} \left\langle \left| \int \sigma^z(\mathbf{r}) e^{-i\mathbf{q} \cdot \mathbf{r}} d\mathbf{r} \right|^2 \right\rangle \\ &\sim \frac{1}{N_{\text{spin}}} \int G_2(\mathbf{r}) e^{-i(\mathbf{q} - \mathbf{Q}_c) \cdot \mathbf{r}} d\mathbf{r} \\ &\sim L^{-2x_{\text{SDW}}} \Phi_2[L(\mathbf{q} - \mathbf{Q}_c), \xi^{-1}L]. \end{aligned} \quad (6)$$

A similar argument can also be made for the four-point correlation function $G_4(\mathbf{r}_1, \mathbf{r}_2, \mathbf{r}_3, \mathbf{r}_4) = \langle \phi_c(\mathbf{r}_1) \phi_c(\mathbf{r}_2) \phi_c(\mathbf{r}_3) \phi_c(\mathbf{r}_4) \rangle$, leading to

$$\langle |M_{\mathbf{q}}|^4 \rangle \sim L^{-4x_{\text{SDW}}} \Phi_4[L(\mathbf{q} - \mathbf{Q}_c), \xi^{-1}L]. \quad (7)$$

Thus, near the critical point $T \approx T_{\text{SDW}}$, we find that the Binder parameter associated with the effective ordering wave vector behaves as

$$U_{L_c}^{\text{eff}} \sim \Phi_U[L(\mathbf{Q}_L^{\text{eff}} - \mathbf{Q}_c), \xi^{-1}L]. \quad (8)$$

In the meantime, it is expected $U_{L_c}^{\text{eff}} \rightarrow 2$ (corresponding to the Gaussian distribution for a one-component complex order parameter) and $U_{L_c}^{\text{eff}} \rightarrow 1$ in the high- and low- T limits, respectively. In the above discussion, Ψ_2 , Φ_2 , Φ_4 , and Φ_U are finite-size scaling functions.

It is reasonable to assume that these scaling functions are sufficiently isotropic with respect to small $|\mathbf{Q}_L^{\text{eff}} - \mathbf{Q}_c|$ with an appropriate rescaling along the principle axes if needed [48].

In fact, Z_2 reflection symmetry along the c axis concerning the sign of $Q_{L,3}^{\text{eff}} - Q_3$ is enough for the following discussion. As a wave vector best approximating the true ordering wave vector for a given system size L , we expect $|\mathbf{Q}_L^{\text{eff}} - \mathbf{Q}_c| \sim O(L^{-1})$. Since, the universal scaling functions can be expected as sufficiently slowly varying near the critical point $T \approx T_{\text{SDW}}$, the right-hand side of Eq. (8) is almost a size-independent constant. Therefore, the Binder parameter at the size-dependent effective ordering wave vectors is expected to exhibit a crossing behavior at around $T = T_{\text{SDW}}$.

In the meantime, to determine $T_{\text{IC-C}}$ for the lock-in IC-C transition into a commensurate phase in low fields, or T_c for a direct transition into the same phase in high fields, we use the ordinary the Binder parameter $U_{\mathbf{q}_{\text{com}}} = \langle |M_{\mathbf{q}_{\text{com}}}|^4 \rangle / \langle |M_{\mathbf{q}_{\text{com}}}|^2 \rangle^2$ at the corresponding commensurate wave-vector $\mathbf{q} = \mathbf{q}_{\text{com}} = (0, 0, 2\pi)$.

C. Ordering wave vector and the phase diagram

Below, we discuss the details of the phase diagram for $\kappa = 0.1$ [Fig. 2(b)], which is obtained by the simulation for $T \gtrsim 0.45|J_1|$. We first focus on the behavior of the ordering wave vector (Fig. 3). At low fields, we observe that the ordering wave vector $\mathbf{Q}_L^{\text{eff}} = (0, 0, Q_{L,3}^{\text{eff}})$ at $T = T_{\text{SDW}}$ deviates slightly, but clearly, from $\mathbf{q}_{\text{com}} = (0, 0, 2\pi)$. Below T_{SDW} , $\mathbf{Q}_L^{\text{eff}}$ slowly drifts towards $\mathbf{q}_{\text{com}} = (0, 0, 2\pi)$ as further lowering T . Roughly speaking, the ordering wave vector changes more rapidly for a larger magnetic field. The observed steplike behavior of $\mathbf{Q}_L^{\text{eff}}$ is simply due to the finite-size discretization of the wave vector [e.g., $\Delta Q_{L,3}^{\text{eff}}/(2\pi) = 0.003125$ for $L_c = 320$], which also causes spurious peaks in C at wildly size-dependent temperatures (Fig. 3). Considering the wide range of the system sizes we investigated, the most natural interpretation is that the change in the wave vector in thermodynamic limit, $\mathbf{Q}(T) = \lim_{L \rightarrow \infty} \mathbf{Q}_L^{\text{eff}}(T)$, is (quasi-)continuous towards \mathbf{q}_{com} . When $\mathbf{Q}_L^{\text{eff}}(T)$ changes from one value to another as a function of T in a finite-size system, a disordering effect appears at large distance due to the mismatch between an ideal wave length and the system size. The mismatch-induced disordering effect causes a spurious

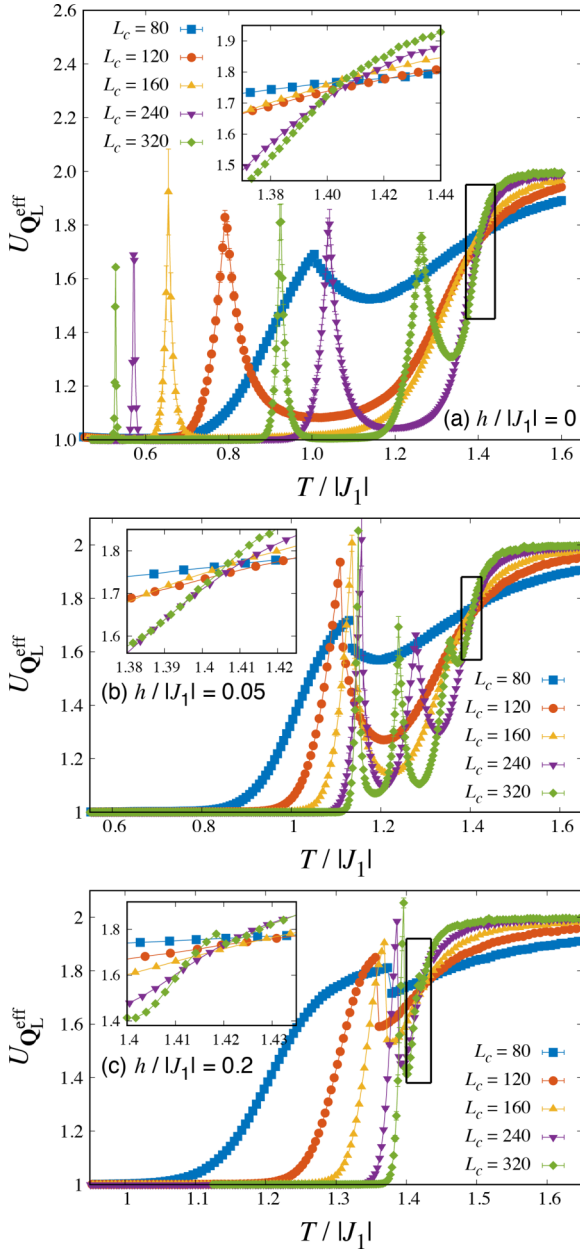


FIG. 4. Monte Carlo results of the modified Binder parameter $U_{Q_L}^{\text{eff}}$ [Eq. (3)] for (a) $h/|J_1| = 0$, (b) $h/|J_1| = 0.05$, and (c) $h/|J_1| = 0.2$. The insets show enlarged views near $T = T_{\text{SDW}}$.

spiky peak in $U_{Q_L}^{\text{eff}}$ (Fig. 4) and interfere with high-precision determination of T_{SDW} because it also affects the behavior of $U_{Q_L}^{\text{eff}}$ near T_{SDW} , making the trend of the crossing less systematic. Therefore, we treat the first crossing points of $U_{Q_L}^{\text{eff}}$ for $(L_c, 2L_c) = (80, 160)$, $(120, 240)$, and $(160, 320)$ simply on an equal footing, which nonetheless allows for determining the transition point of the SDW ordering to the satisfactory precision, e.g., $T_{\text{SDW}}/|J_1| = 1.407(5)$, $1.406(1)$, and $1.41(2)$ for $h/|J_1| = 0, 0.05$, and 0.2 , respectively (Fig. 4). The estimated T_{SDW} roughly coincides with the highest- T peak in the specific heat (see Fig. 3).

At low temperatures, the ordering wave vector is pinned at $\mathbf{q}_{\text{com}} = (0, 0, 2\pi)$, corresponding to a three-sublattice

ordered phase. At low fields, the low- T phase appears through a lock-in IC-C transition where the translational symmetry along the c axis, which is broken in the SDW state, is restored. By analyzing the behavior of $U_{\mathbf{q}_{\text{com}}}$, we find that $T_{\text{IC-C}}/|J_1|$ increases rapidly with h (see Fig. 2), e.g., $T_{\text{IC-C}}/|J_1| = 0.52(1)$, $1.15(3)$, and $1.397(3)$ for $h/|J_1| = 0, 0.05$, and 0.2 , respectively. Since T_{SDW} is nearly constant in h , this observation means that the SDW phase shrinks rather rapidly with increasing h , and above a magnetic field induced multicritical point $h_{\text{LP}} \simeq 0.2|J_1| \simeq 0.17h_{\text{sat}}$, where $h_{\text{sat}} = 6(J_2 + J_3)$ is the saturation field, no incommensurate phase is found. The estimated IC-C transition temperatures coincide with the temperatures at which the finite-size ordering wave vector reaches $\mathbf{Q}_L^{\text{eff}} = \mathbf{q}_{\text{com}}$ at each field, as expected. Also, $\langle |M_{\mathbf{q}_{\text{com}}}|^2 \rangle$ increases rapidly around the estimated temperatures and becomes almost size independent at lower temperatures (Fig. 5). Although the IC-C transitions studied in the present MC work tend to exhibit typical features of a first-order transition, such as the correction in the finite-size transition temperature varying as $\sim 1/L^3$, they may be a spurious behavior caused by discrete wave vectors in finite-size systems.

For $T < T_{\text{IC-C}}$, the two main candidates for the three-sublattice order are the FIM state and the PDA state, similar to the case in triangular lattice antiferromagnetic Ising models [49–54]. In the FIM state, each spin chain has a ferromagnetic order and different spin chains takes the three-sublattice $\uparrow\uparrow\downarrow$ structure. In the PDA phase, the spin chains in the first and the second sublattices have a ferromagnetic order with spin- \uparrow and spin- \downarrow , respectively, with the spin chains in the third sublattice disordered. A convenient indicator for a finite-size calculation is

$$C_6 = \frac{\langle M_{\mathbf{q}_{\text{com}}}^6 \rangle}{\langle |M_{\mathbf{q}_{\text{com}}}|^6 \rangle}, \quad (9)$$

which takes $C_6 > 0$ ($C_6 < 0$) for the FIM (PDA) state [51]. For $h = 0$, we confirm the PDA state below $T_{\text{IC-C}}$ (Fig. 5). For $h \neq 0$, we find the FIM state at low T down to $h/|J_1| = 0.025$, implying that the observed PDA state is extremely fragile against the magnetic field. The confirmed PDA state in zero field should be distinguished from the previous claim of the same state in CCO below $\simeq 25$ K, which has now been known to be the SDW state [14]. Nevertheless, our result suggests that the PDA state may be stabilized when the wavelength of the SDW state goes to infinity in equilibrium. We also mention that we find no evidence of an additional order-order transition at low T as reported in CCO [36], at least for $T \gtrsim 0.45|J_1|$. The FIM phase in a magnetic field yields the $1/3$ magnetization plateau [35]. At high fields, we find a direct transition into the FIM phase without the intervening SDW phase. We find that the transition is of the first order, which is consistent with the Z_3 symmetry breaking in $d = 3$, as in the three-state Potts model [55,56].

V. GINZBURG-LANDAU THEORY

Finally, for a more universal description of the commensurate and incommensurate phases in CCO and similar materials, we consider a GL theory. As will be shown below, the theory is essentially in the same form as that for the ANNNI model [57,58]. Interestingly, however, the GL theory

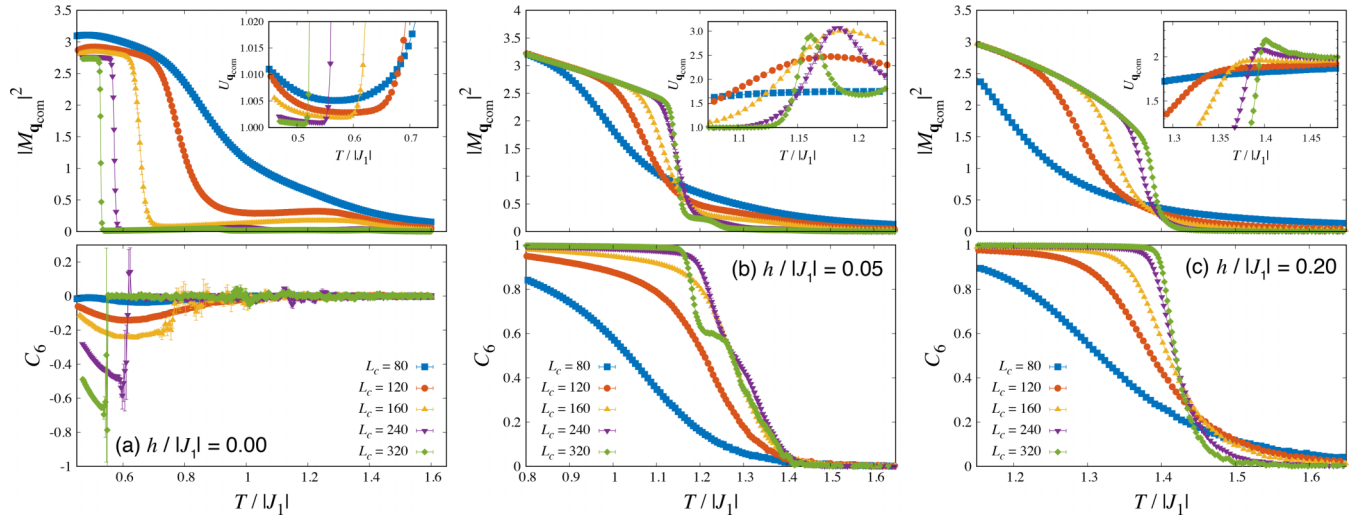


FIG. 5. Monte Carlo results of the square of the commensurate order parameter (upper panels) and the C_6 indicator to distinguish between the partially disordered antiferromagnetic (PDA) state ($C_6 < 0$) and the ferrimagnetic (FIM) state ($C_6 > 0$) (lower panels) for (a) $h/|J_1| = 0$, (b) $h/|J_1| = 0.05$, and (c) $h/|J_1| = 0.2$. The insets show enlarged views of the Binder parameter for the commensurate order parameter near $T = T_{\text{IC-C}}$.

for ANNNI-like models in magnetic fields [59] has yet been thoroughly discussed in the literature, despite its experimental relevance in many contexts.

We use a complex order parameter $\psi(\mathbf{r}) \sim e^{-i\mathbf{q}_{\text{com}} \cdot \mathbf{r}} \sigma^z(\mathbf{r})$, $\mathbf{q}_{\text{com}} = (0, 0, 2\pi)$, which can be formally introduced by using the Hubbard-Stratonovich transformation. $\psi(\mathbf{r})$ describes the local three-sublattice order in a coarse-grained way, which can be either the FIM order or the PDA order depending on the phase factor. For $h = 0$, we find the following GL Hamiltonian:

$$\mathcal{H}_{h=0} = \int d^3\mathbf{r} \left[\frac{1}{2} t |(\nabla - i\boldsymbol{\epsilon})\psi(\mathbf{r})|^2 + t |\psi(\mathbf{r})|^2 + u_4 |\psi(\mathbf{r})|^4 + u_6 |\psi(\mathbf{r})|^6 + v_6 [(\psi(\mathbf{r})^6 + \psi^*(\mathbf{r})^6)] \right], \quad (10)$$

where t , u_4 , u_6 , and v_6 are GL coefficients and $\boldsymbol{\epsilon} = (0, 0, \epsilon)$. A crucial point of the present theory is that the wave-vector \mathbf{q}_{com} of the local order described by $\psi(\mathbf{r})$ is slightly shifted from the minima $\mathbf{q} = \pm \mathbf{q}_{\text{min}}$ of the Fourier-transform $J(\mathbf{q})$ of the exchange interactions in such a way that $\mathbf{q}_{\text{min}} = \mathbf{q}_{\text{com}} + \boldsymbol{\epsilon}$. For this reason, $\mathcal{H}_{h=0}$ includes the vector potential-like (but constant) contribution $-i\boldsymbol{\epsilon}$ in the gradient term. $\mathcal{H}_{h=0}$ also includes the six-order term (v_6) as the leading umklapp term, the order of which is determined by the size of the magnetic sublattice of the commensurate order and time-reversal symmetry; a factor of 3 comes from $3\mathbf{q}_{\text{com}} \equiv 0$ and time-reversal symmetry requires another factor of 2.

As is clear from the origin, the gradient term acts as adding a momentum $\boldsymbol{\epsilon}$ to ψ , in favor of the three-sublattice long-wavelength SDW state $\langle \psi(\mathbf{r}) \rangle \sim (\text{const.}) \times e^{i\boldsymbol{\epsilon} \cdot \mathbf{r}}$. However, on one hand, although the SDW state appears to benefit from the exchange energy, the sinusoidal modulation made of localized Ising-like moments would require an entropy contribution to the free energy. On the other hand, the commensurate three-sublattice ordered state, $\langle \psi(\mathbf{r}) \rangle \sim \text{const.}$, may not appear to acquire the full energy gain of the exchange interaction but the

state is quite compatible with the Ising anisotropy. In the GL theory (10), the umklapp term plays the role of the relative entropy contribution related with the Ising anisotropy. Although the commensurate state may be favored by the umklapp term by adjusting its constant phase factor, the incommensurate SDW states generally gain no corresponding contribution because of the phase cancellation in the integral over the space. In fact, we could rederive the GL theory in terms of $\phi_c(\mathbf{r}) \sim \sigma^z(\mathbf{r}) e^{-i\mathbf{q}_{\text{min}} \cdot \mathbf{r}}$ instead of $\psi(\mathbf{r}) \sim \sigma^z(\mathbf{r}) e^{-i\mathbf{q}_{\text{com}} \cdot \mathbf{r}}$, and the result is an ordinary ϕ_c^4 theory for the one-component complex order parameter without umklapp terms as long as \mathbf{q}_{min} is incommensurate. Hence, the key role in the GL theory (10) is played by the competition between the gradient and the umklapp terms favoring incommensuration and commensuration, respectively. Thus, although somewhat different in appearance, the Hamiltonian of this system (1) realizes essentially the same situation as in the classic ANNNI model [58].

At $T = T_{\text{SDW}}$, critical fluctuations renders $\psi(\mathbf{r})$ nonzero with the additional momentum $\boldsymbol{\epsilon}$, resulting in the SDW state with the ordering wave-vector $\mathbf{Q} = \mathbf{q}_{\text{com}} + \boldsymbol{\epsilon} = \mathbf{q}_{\text{min}}$. In other words, we expect a condensation of the softest mode $\phi_c(\mathbf{r}) \sim \sigma^z(\mathbf{r}) e^{-i\mathbf{q}_{\text{min}} \cdot \mathbf{r}}$ rather than $\psi(\mathbf{r}) \sim \sigma^z(\mathbf{r}) e^{-i\mathbf{q}_{\text{com}} \cdot \mathbf{r}}$. The SDW transition breaks the translation symmetry along the c -axis but the corresponding wavelength is very large and incommensurate, suggesting emergent U(1) symmetry for the critical fluctuation. In the GL theory, the umklapp v_6 term has no effect for the incommensurate SDW state, and the 3D XY universality class is indeed expected. The observed main peak of the specific heat, which exhibits a sign of smearing [Fig. 3(a)], is consistent with the negative exponent $\alpha = -0.0146(8) < 0$ for the XY universality class [60].

For $T < T_{\text{SDW}}$, the competition between the gradient term and the umklapp term sets in, which affects the phase factor of $\langle \psi(\mathbf{r}) \rangle$, thereby $\mathbf{Q}(T < T_{\text{SDW}})$. To see this, we may write $\psi(\mathbf{r}) = A(\mathbf{r})e^{i\theta(\mathbf{r})}$ and apply a mean-field decoupling for the massive amplitude fluctuation (“Higgs”) mode $\delta A(\mathbf{r}) = A(\mathbf{r}) - \langle A \rangle$ and the phase mode $\theta(\mathbf{r})$ [58]. The result is the

following sine-Gordon model for $\theta(\mathbf{r})$,

$$\mathcal{H}'_{h=0,\theta} = \langle A \rangle^2 \int d^3\mathbf{r} \left[\frac{1}{2} [\nabla\theta(\mathbf{r}) - \boldsymbol{\epsilon}]^2 + 2\langle A \rangle^4 v_6 \cos 6\theta(\mathbf{r}) \right]. \quad (11)$$

The gradient term tends to drift the phase, which can lead to a plethora of soliton lattices through the competition against the cosine term [58,61], in good agreement with our mean-field and MC studies. In the meantime because the order parameter amplitude $\langle A \rangle$ increases as T is lowered below T_{SDW} , the strength of the cosine term is enhanced. Consequently, the model at low T is expected to undergo a lock-in transition eventually. For $v_6 > 0$ ($v_6 < 0$), the phase is locked in at $\theta = 2n\pi/6$ [$\theta = (2n+1)\pi/6$] with an integer $0 \leq n < 6$, corresponding to the FIM ($\uparrow\uparrow\downarrow$ or $\downarrow\downarrow\uparrow$) state and the PDA state [49–54], respectively. Our mean-field calculation implies $v_6 > 0$ whereas our unbiased MC simulation suggests $v_6 < 0$ in zero field, though the subtle discrepancy does not require serious attention as v_6 is generated through fluctuations.

For $h \neq 0$, the uniform $\mathbf{q} = 0$ component $m(\mathbf{r})$ is allowed by symmetry and may be induced by the magnetic field. Consequently, in addition to v_6 , a *lower-order* umklapp term appears in the GL Hamiltonian. We find

$$\Delta\mathcal{H}_{0-\mathbf{q}_{\text{com}}} \simeq \int d^3\mathbf{r} w_4 m(\mathbf{r}) [\psi(\mathbf{r})^3 + \psi^*(\mathbf{r})^3], \quad (12)$$

as the leading-order contribution with the new coupling constant w_4 . The total effective GL Hamiltonian for $h \neq 0$ is

$$\mathcal{H}_{h \neq 0, \psi, m} = \mathcal{H}_{h=0, \psi} + \mathcal{H}_{\mathbf{q}=0, m} + \Delta\mathcal{H}_{0-\mathbf{q}_{\text{com}}}, \quad (13)$$

where $\mathcal{H}_{\mathbf{q}=0, m} = \int d^3\mathbf{r} [\frac{1}{2} [c\nabla m(\mathbf{r})]^2 + \mu^2 m(\mathbf{r})^2 - hm(\mathbf{r})]$ is the noninteracting part for $m(\mathbf{r})$ with $c > 0$ and $\mu^2 > 0$ being the gapped spin-wave parameters near $\mathbf{q} = 0$. By a similar mean-field decoupling as in the $h = 0$ case, we find a new term in the sine-Gordon model,

$$\Delta\mathcal{H}'_{0-\mathbf{q}_{\text{com}}, \theta} = 2w_4 \langle m \rangle \langle A \rangle^3 \int d^3\mathbf{r} \cos 3\theta(\mathbf{r}). \quad (14)$$

The field induced umklapp term has the following consequences. First, because of the reduced symmetry in the θ space, only a subset of the FIM states is favored by $\Delta\mathcal{H}'_{0-\mathbf{q}_{\text{com}}, \theta}$ among the three-sublattice ordered states. Depending on the sign of w_4 , the favored states are $\uparrow\uparrow\downarrow$ or $\downarrow\downarrow\uparrow$, each of which is threefold degenerate, although $\uparrow\uparrow\downarrow$ is naturally anticipated for $h > 0$. Second, as the prefactor is $\propto \langle A \rangle^3$ as opposed to $\propto \langle A \rangle^6$ in zero field, the strength of the field induced umklapp term is expected to grow faster for $T < T_{\text{SDW}}$. Moreover, since the prefactor is $\propto \langle m \rangle$, we expect that this trend is further enhanced for larger h . Therefore, the region of the incommensurate SDW microphases is expected to become narrower for larger h , in excellent agreement with our MC results (Fig. 2). Third, considering that our MC simulation shows the PDA state at $h = 0$ below $T_{\text{IC-C}}$, the zero- and the field induced umklapp terms ($\sim \cos 6\theta$, $\cos 3\theta$, respectively) must compete against each other in the present system. The competition opens a possibility of a kind of mixed phase below $T_{\text{IC-C}}$, though our MC results shows no evidence down to an extremely low field, $h/|J_1| = 0.025$. Finally, near $T = T_{\text{SDW}}$, the present GL

theory suggests the condensation of the softest mode $\phi_c(\mathbf{r}) \sim \sigma^z(\mathbf{r}) e^{-i\mathbf{q}_{\text{min}} \cdot \mathbf{r}}$ rather than $\psi(\mathbf{r}) \sim \sigma^z(\mathbf{r}) e^{-i\mathbf{q}_{\text{com}} \cdot \mathbf{r}}$ at the SDW transition, as in the case of zero magnetic field. Hence, we expect the emergent $U(1)$ symmetry at $T = T_{\text{SDW}}$ also for $h \neq 0$ because umklapp terms disappear from the GL theory in terms of the incommensurate critical mode ϕ_c . The theory, thus, predicts $\mathbf{Q}(T = T_{\text{SDW}}) = \mathbf{q}_{\text{min}}$ for any magnetic field, which is indeed consistent with our MC results at low magnetic fields. However, the simulation closer to the magnetic field-induced multicritical point $h_{\text{LP}} \simeq 0.2|J_1|$ might point to a deviation from this behavior, suggesting that $\mathbf{Q}(T = T_{\text{SDW}})$ approaches towards \mathbf{q}_{com} for the larger systems we investigated [Fig. 3(c)]. This observation may be an indication that the multicritical point is a Lifshitz point induced by a magnetic field.

VI. SUMMARY AND OUTLOOK

To summarize, we presented the magnetic phase diagram in equilibrium of the 3D spin model for the frustrated quasi-one-dimensional triangular Ising antiferromagnet $\text{Ca}_3\text{Co}_2\text{O}_6$. We identified the region of incommensurate SDW microphases in a magnetic field (Fig. 2). We found the deformation of SDW microphases as a function of T , characterized by the temperature dependence of the ordering wave-vector $\mathbf{Q}(T)$, which occurs much more rapidly in a magnetic field than in zero field (Fig. 3). The deformation eventually leads to the IC-C transition into the PDA (FIM) state for $h = 0$ ($h \neq 0$). Between the PDA and the FIM phases, there may be a mixed phase in an extremely low-field regime, although not confirmed in this paper. The GL theory we derived includes different symmetry-allowed umklapp terms for $h = 0$ and $h \neq 0$. The GL theory allowed for further deriving an effective sine-Gordon model that provides a qualitative explanation of the observed magnetic field induced deformation of the SDW microphases. Moreover, these effective theories demonstrate that the present system can be seen as an incarnation of the classic ANNNI model [58], despite different appearance of the lattice structure and the more complicated network of the exchange interactions.

Finally, we discuss the relation between the theoretical phase diagram in this paper and the previous experiments. As mentioned in the Introduction, the material is known for the intriguing combination of the slow relaxation phenomena and the long-wavelength SDW order. As the recent field-cooling study suggested [35], the slow relaxation at low temperature may be greatly influenced by the cooling process passing through the low-field SDW phase at intermediate temperature. To verify the conjectured relation experimentally, the challenge is that experiments under equilibrium conditions are known to be notoriously difficult for $\text{Ca}_3\text{Co}_2\text{O}_6$. For example, resonant x-ray experiments reported a field induced IC-C transition at 5 K [17], which is unfortunately most likely nonequilibrium because the temperature is too low. However, at intermediate temperatures above T_{SF} , there are some experiments that seem to capture the desired physics of the field induced deformation of the SDW phase and the IC-C transition. For example, μSR measurements at 20 K reported a magnetic field induced phase transition at around 0.4 T [62]. Although the original interpretation of the result suggested

a PDA-FIM transition, the obtained phase boundary is very similar to the SDW-FIM transition line shown in the present paper. Since the SDW phase was not confirmed back then, it is quite possible that the anomaly in the μ SR experiment is the sign of the IC-C transition induced by the magnetic field. We also note that a similar phase diagram was obtained also by weak anomaly in the magnetic entropy change [63]. We, thus, believe that further experiments studying the field induced IC-C transition in $\text{Ca}_3\text{Co}_2\text{O}_6$, such as neutron scattering and other spectroscopies focusing on the low-field regime, will be very promising, especially when combined with the recently proposed field-cooling protocol [35]. Such experiments

may provide further insights in the peculiar slow dynamics and out-of-equilibrium behaviors in $\text{Ca}_3\text{Co}_2\text{O}_6$ and related materials.

ACKNOWLEDGMENTS

I am grateful for valuable discussions with V. Zapf, X. Ding, I. Nekrashevich, and C. Batista. I acknowledge support from the NSFC (Grants No. 11950410507, No. 12074246, and No. U2032213) and MOST (Grant No. 2016YFA0300501) research programs.

-
- [1] *Introduction to Frustrated Magnetism: Materials, Experiments, Theory*, edited by C. Lacroix, P. Mendels, and F. Mila (Springer-Verlag, Heidelberg, 2011).
- [2] A. N. Bogdanov and C. Panagopoulos, *Nat. Rev. Phys.* **2**, 492 (2020).
- [3] S. T. Bramwell and M. J. P. Gingras, *Science* **294**, 1495 (2001).
- [4] C. Paulsen, M. J. Jackson, E. Lhotel, B. Canals, D. Prabhakaran, K. Matsuhira, S. R. Giblin, and S. T. Bramwell, *Nat. Phys.* **10**, 135 (2014).
- [5] S. T. Bramwell and M. J. Harris, *J. Phys.: Condens. Matter* **32**, 374010 (2020).
- [6] T. Okubo, S. Chung, and H. Kawamura, *Phys. Rev. Lett.* **108**, 017206 (2012).
- [7] A. O. Leonov and M. Mostovoy, *Nat. Commun.* **6**, 8275 (2015).
- [8] P. Bak, *Rep. Prog. Phys.* **45**, 587 (1982).
- [9] W. Selke, *Phys. Rep.* **170**, 213 (1988).
- [10] A. Fert, N. Reyren, and V. Cros, *Nat. Rev. Mater.* **2**, 17031 (2017).
- [11] Y. B. Kudasov, *Phys. Rev. Lett.* **96**, 027212 (2006).
- [12] H. Fjellvåg, E. Gulbrandsen, S. Aasland, A. Olsen, and B. C. Hauback, *J. Solid State Chem.* **124**, 190 (1996).
- [13] S. Aasland, H. Fjellvåg, and B. Hauback, *Solid State Commun.* **101**, 187 (1997).
- [14] H. Kageyama, K. Yoshimura, K. Kosuge, H. Mitamura, and T. Goto, *J. Phys. Soc. Jpn.* **66**, 1607 (1997).
- [15] H. Kageyama, K. Yoshimura, K. Kosuge, M. Azuma, M. Takano, H. Mitamura, and T. Goto, *J. Phys. Soc. Jpn.* **66**, 3996 (1997).
- [16] S. Agrestini, L. C. Chapon, A. Daoud-Aladine, J. Schefer, A. Gukasov, C. Mazzoli, M. R. Lees, and O. A. Petrenko, *Phys. Rev. Lett.* **101**, 097207 (2008).
- [17] C. Mazzoli, A. Bombardi, S. Agrestini, and M. R. Lees, *Physica B* **404**, 3042 (2009).
- [18] S. Agrestini, C. Mazzoli, A. Bombardi, and M. R. Lees, *Phys. Rev. B* **77**, 140403(R) (2008).
- [19] T. Moyoshi and K. Motoya, *J. Phys. Soc. Jpn.* **80**, 034701 (2011).
- [20] C. L. Fleck, M. R. Lees, S. Agrestini, G. J. McIntyre, and O. A. Petrenko, *Europhys. Lett.* **90**, 67006 (2010).
- [21] J. A. M. Paddison, S. Agrestini, M. R. Lees, C. L. Fleck, P. P. Deen, A. L. Goodwin, J. R. Stewart, and O. A. Petrenko, *Phys. Rev. B* **90**, 014411 (2014).
- [22] K. Motoya, T. Kihara, H. Nojiri, Y. Uwatoko, M. Matsuda, and T. Hong, *J. Phys. Soc. Jpn.* **87**, 114703 (2018).
- [23] Y. Kamiya and C. D. Batista, *Phys. Rev. Lett.* **109**, 067204 (2012).
- [24] B. Leedahl, M. Sundermann, A. Amorese, A. Severing, H. Gretarsson, L. Zhang, A. C. Komarek, A. Maignan, M. W. Haverkort, and L. H. Tjeng, *Nat. Commun.* **10**, 5447 (2019).
- [25] A. Maignan, C. Michel, A. C. Masset, C. Martin, and B. Raveau, *Eur. Phys. J. B* **15**, 657 (2000).
- [26] V. Hardy, M. R. Lees, O. A. Petrenko, D. McK. Paul, D. Flahaut, S. Hébert, and A. Maignan, *Phys. Rev. B* **70**, 064424 (2004).
- [27] A. Maignan, V. Hardy, S. Hbert, M. Drillon, M. R. Lees, O. Petrenko, D. M. K. Paul, and D. Khomskii, *J. Mater. Chem.* **14**, 1231 (2004).
- [28] J. W. Kim, E. D. Mun, X. Ding, A. Hansen, M. Jaime, N. Harrison, H. T. Yi, Y. Chai, Y. Sun, S. W. Cheong, and V. S. Zapf, *Phys. Rev. B* **98**, 024407 (2018).
- [29] X. Y. Yao, S. Dong, and J. M. Liu, *Phys. Rev. B* **73**, 212415 (2006).
- [30] X. Yao, S. Dong, H. Yu, and J. Liu, *Phys. Rev. B* **74**, 134421 (2006).
- [31] Y. B. Kudasov, A. S. Korshunov, V. N. Pavlov, and D. A. Maslov, *Phys. Rev. B* **78**, 132407 (2008).
- [32] M. H. Qin, K. F. Wang, and J. M. Liu, *Phys. Rev. B* **79**, 172405 (2009).
- [33] R. Soto, G. Martínez, M. N. Baibich, J. M. Florez, and P. Vargas, *Phys. Rev. B* **79**, 184422 (2009).
- [34] M. Žukovič, L. Mižišin, and A. Bobák, *Phys. Lett. A* **376**, 1731 (2012).
- [35] I. Nekrashevich, X. Ding, F. Balakirev, H. T. Yi, S.-W. Cheong, L. Civale, Y. Kamiya, and V. S. Zapf, *Phys. Rev. B* **105**, 024426 (2022).
- [36] S. Agrestini, C. L. Fleck, L. C. Chapon, C. Mazzoli, A. Bombardi, M. R. Lees, and O. A. Petrenko, *Phys. Rev. Lett.* **106**, 197204 (2011).
- [37] M. Seul and D. Andelman, *Science* **267**, 476 (1995).
- [38] V. Hardy, V. Caignaert, O. Pérez, L. Hervé, N. Sakly, B. Raveau, M. M. Seikh, and F. Damay, *Phys. Rev. B* **98**, 144414 (2018).
- [39] S. Niitaka, K. Yoshimura, K. Kosuge, M. Nishi, and K. Kakurai, *Phys. Rev. Lett.* **87**, 177202 (2001).
- [40] R. Frésard, C. Laschinger, T. Kopp, and V. Eyert, *Phys. Rev. B* **69**, 140405(R) (2004).
- [41] G. Allodi, P. Santini, S. Carretta, S. Agrestini, C. Mazzoli, A. Bombardi, M. R. Lees, and R. De Renzi, *Phys. Rev. B* **89**, 104401 (2014).

- [42] L. C. Chapon, *Phys. Rev. B* **80**, 172405 (2009).
- [43] K. Hukushima and K. Nemoto, *J. Phys. Soc. Jpn.* **65**, 1604 (1996).
- [44] D. Landau and K. Binder, *A Guide to Monte Carlo Simulations in Statistical Physics*, 5th ed. (Cambridge University Press, Cambridge, UK, 2021).
- [45] A. Gendiar and T. Nishino, *Phys. Rev. B* **71**, 024404 (2005).
- [46] K. Zhang and P. Charbonneau, *Phys. Rev. Lett.* **104**, 195703 (2010).
- [47] K. Zhang and P. Charbonneau, *Phys. Rev. B* **83**, 214303 (2011).
- [48] J. Cardy, *Scaling and Renormalization in Statistical Physics* (Cambridge University Press, Cambridge, UK, 1996).
- [49] D. Blankschtein, M. Ma, A. N. Berker, G. S. Grest, and C. M. Soukoulis, *Phys. Rev. B* **29**, 5250 (1984).
- [50] S. N. Coppersmith, *Phys. Rev. B* **32**, 1584 (1985).
- [51] S. V. Isakov and R. Moessner, *Phys. Rev. B* **68**, 104409 (2003).
- [52] O. Heinonen and R. G. Petschek, *Phys. Rev. B* **40**, 9052 (1989).
- [53] A. Bunker, B. D. Gaulin, and C. Kallin, *Phys. Rev. B* **48**, 15861 (1993).
- [54] S.-Z. Lin, Y. Kamiya, G.-W. Chern, and C. D. Batista, *Phys. Rev. Lett.* **112**, 155702 (2014).
- [55] H. W. J. Blöte and R. H. Swendsen, *Phys. Rev. Lett.* **43**, 799 (1979).
- [56] W. Janke and R. Villanova, *Nucl. Phys. B* **489**, 679 (1997).
- [57] A. Aharony and P. Bak, *Phys. Rev. B* **23**, 4770 (1981).
- [58] P. Bak and J. von Boehm, *Phys. Rev. B* **21**, 5297 (1980).
- [59] C. S. O. Yokoi, M. D. Coutinho-Filho, and S. R. Salinas, *Phys. Rev. B* **24**, 4047 (1981).
- [60] M. Campostrini, M. Hasenbusch, A. Pelissetto, P. Rossi, and E. Vicari, *Phys. Rev. B* **63**, 214503 (2001).
- [61] P. M. Chaikin and T. C. Lubensky, *Principles of Condensed Matter Physics* (Cambridge University Press, Cambridge, UK, 1995).
- [62] S. Takeshita, T. Goko, J. Arai, and K. Nishiyama, *J. Phys. Chem. Solids* **68**, 2174 (2007).
- [63] P. Lampen, N. S. Bingham, M. H. Phan, H. Srikanth, H. T. Yi, and S. W. Cheong, *Phys. Rev. B* **89**, 144414 (2014).